Supplementary Information

Adjacent dimer epitope of envelope protein as an important region for Zika virus serum neutralization: a computational investigation

Authors:
Carlos Alessandro Fuzo[1,2*]
E-mail: cafuzo@usp.br

Luiz Felipe Lemes de Araujo[1,3]
E-mail: araujolfelipe@usp.br

Rafael de Souza Pontes[1,3]
E-mail: rafaelpontes@usp.br

Patricia Martinez Évora[1,3]
E-mail: patievora@hotmail.com

Rodrigo Guerino Stabeli[1,3]
E-mail: rodrigo.stabeli@fiocruz.br

Affiliations:

[1]Plataforma de Pesquisa em Medicina Translacional , Fundação Oswaldo Cruz - Fiocruz SP, Avenida dos Bandeirantes 3900, Campus USP Ribeirão Preto, São Paulo, Brazil.

[2]Faculdade de Ciências Farmacêuticas de Ribeirão Preto, Universidade de São Paulo, Avenida Bandeirantes 3900, Ribeirão Preto, SP, Brazil.

[3]Departamento de Bioquímica e Imunologia, Faculdade de Medicina de Ribeirão Preto, Universidade de São Paulo, Avenida Bandeirantes 3900, Ribeirão Preto, São Paulo, Brazil.

*Corresponding Author

E-mail:cafuzo@usp.br

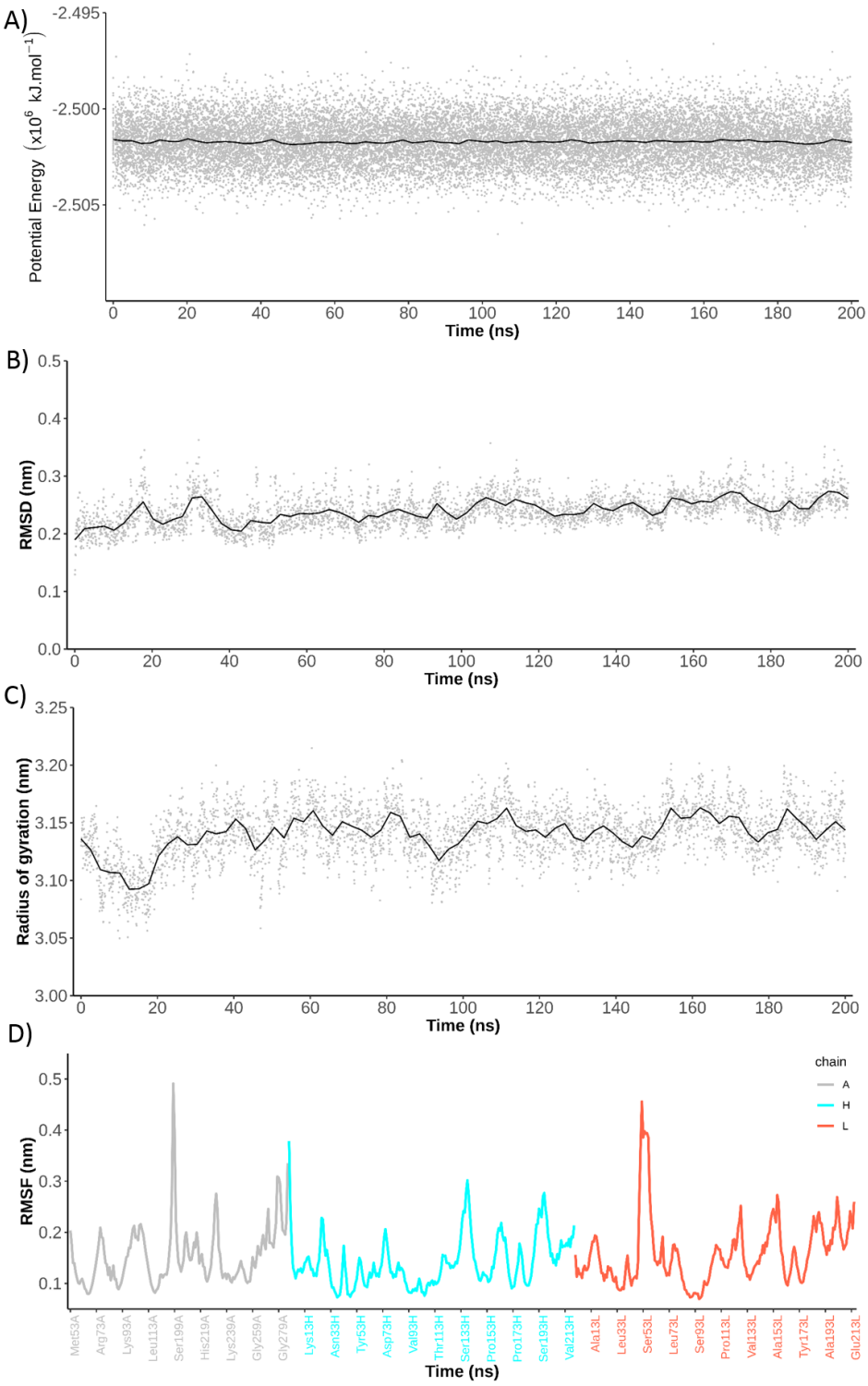

Figure S1 – Diagnostic plots for native system simulation showing the profiles of potential energy (A), root-mean-square deviation after the superposition of C_α atoms to initial structure (B), gyration radius for all atoms (C) and root-mean square fluctuation of C_α atoms from 100 to 200 ns (D).

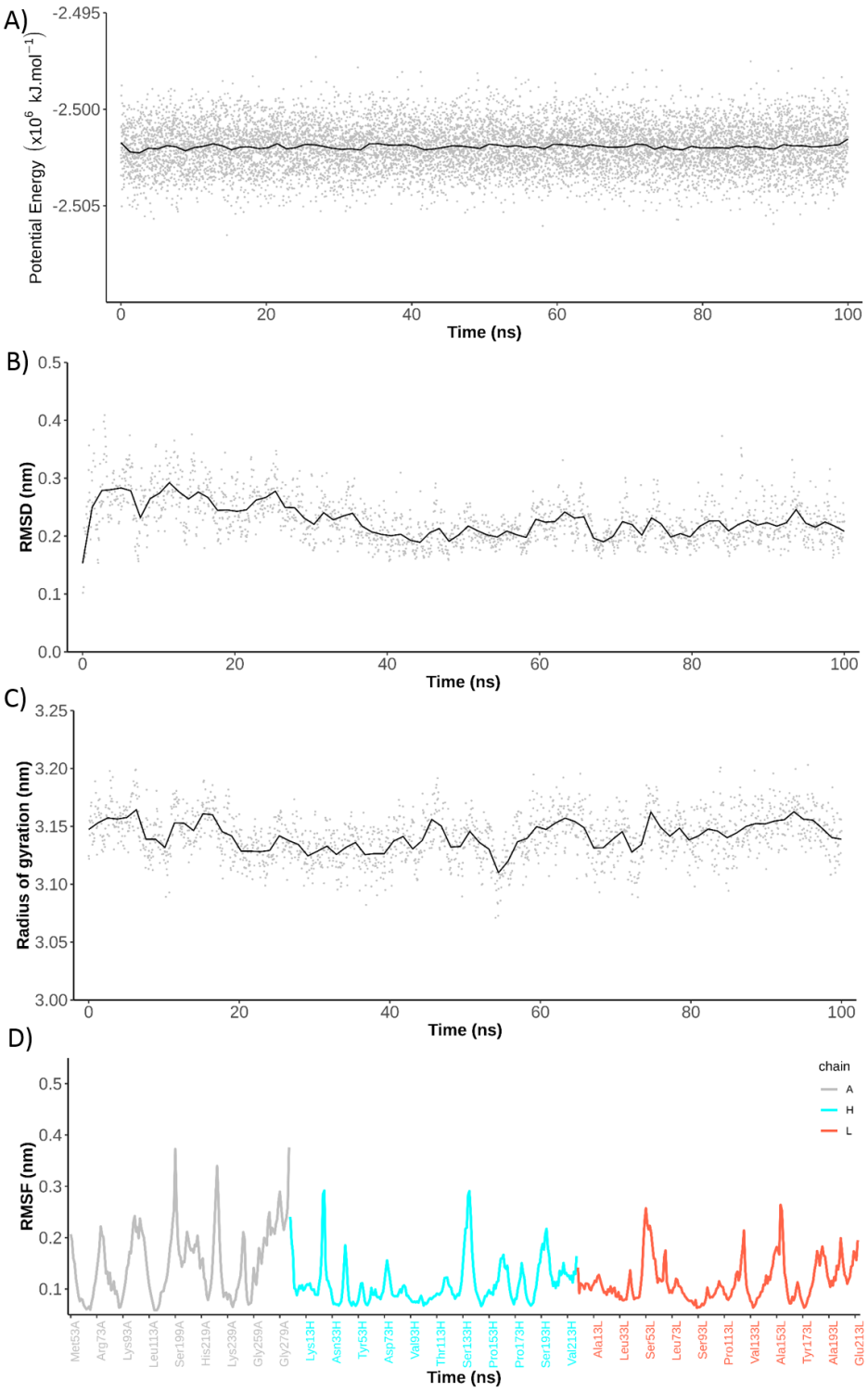

Figure S2 – Diagnostic plots for Asp67Ala system simulation showing the profiles of potential energy (A), root-mean-square deviation after the superposition of C_α atoms to initial structure (B), gyration radius for all atoms (C) and root-mean square fluctuation of C_α atoms from 80 to 100 ns (D).

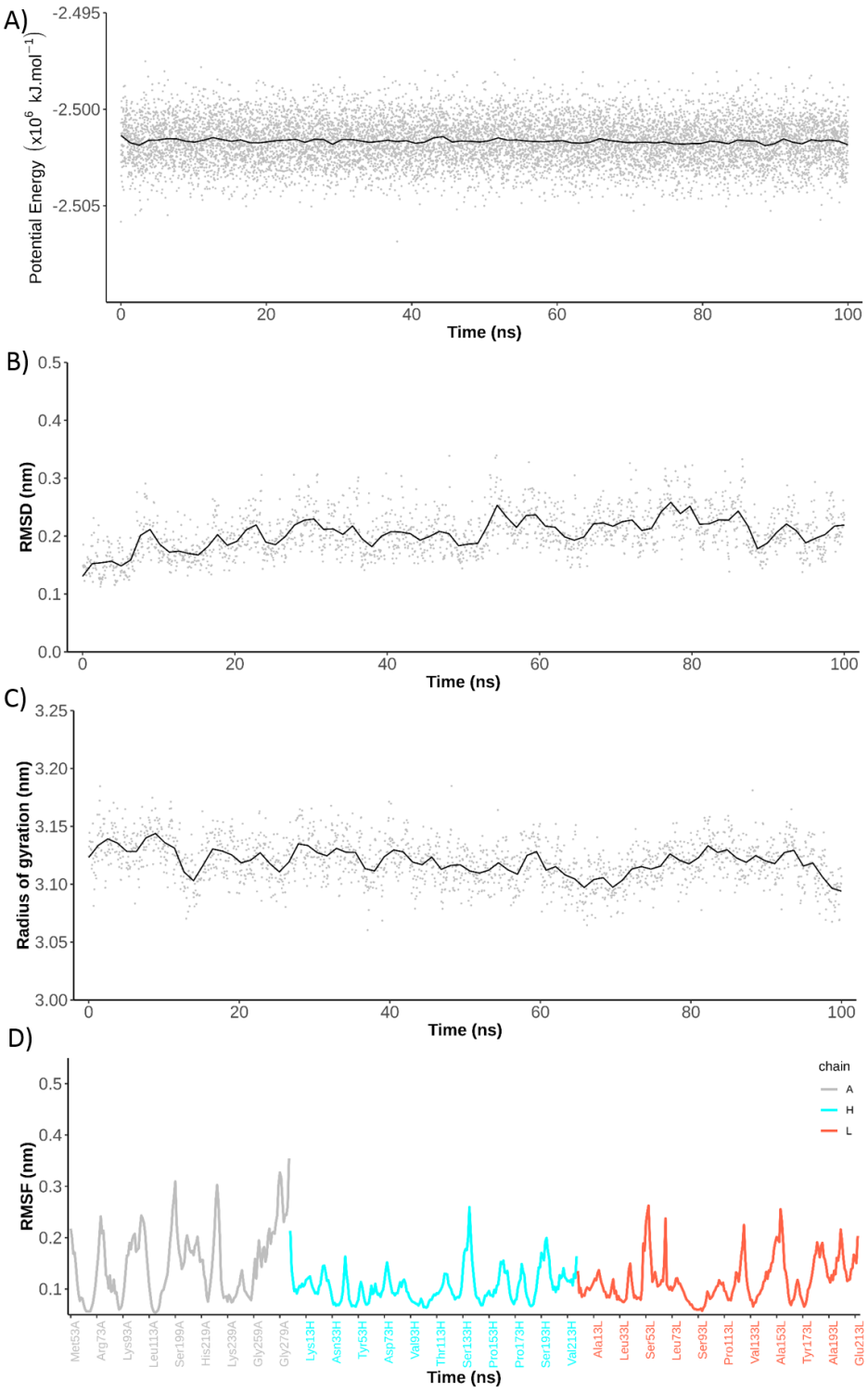

Figure S3 – Diagnostic plots for Gln89Ala system simulation showing the profiles of potential energy (A), root-mean-square deviation after the superposition of C_α atoms to initial structure (B), gyration radius for all atoms (C) and root-mean square fluctuation of C_α atoms from 80 to 100 ns (D).

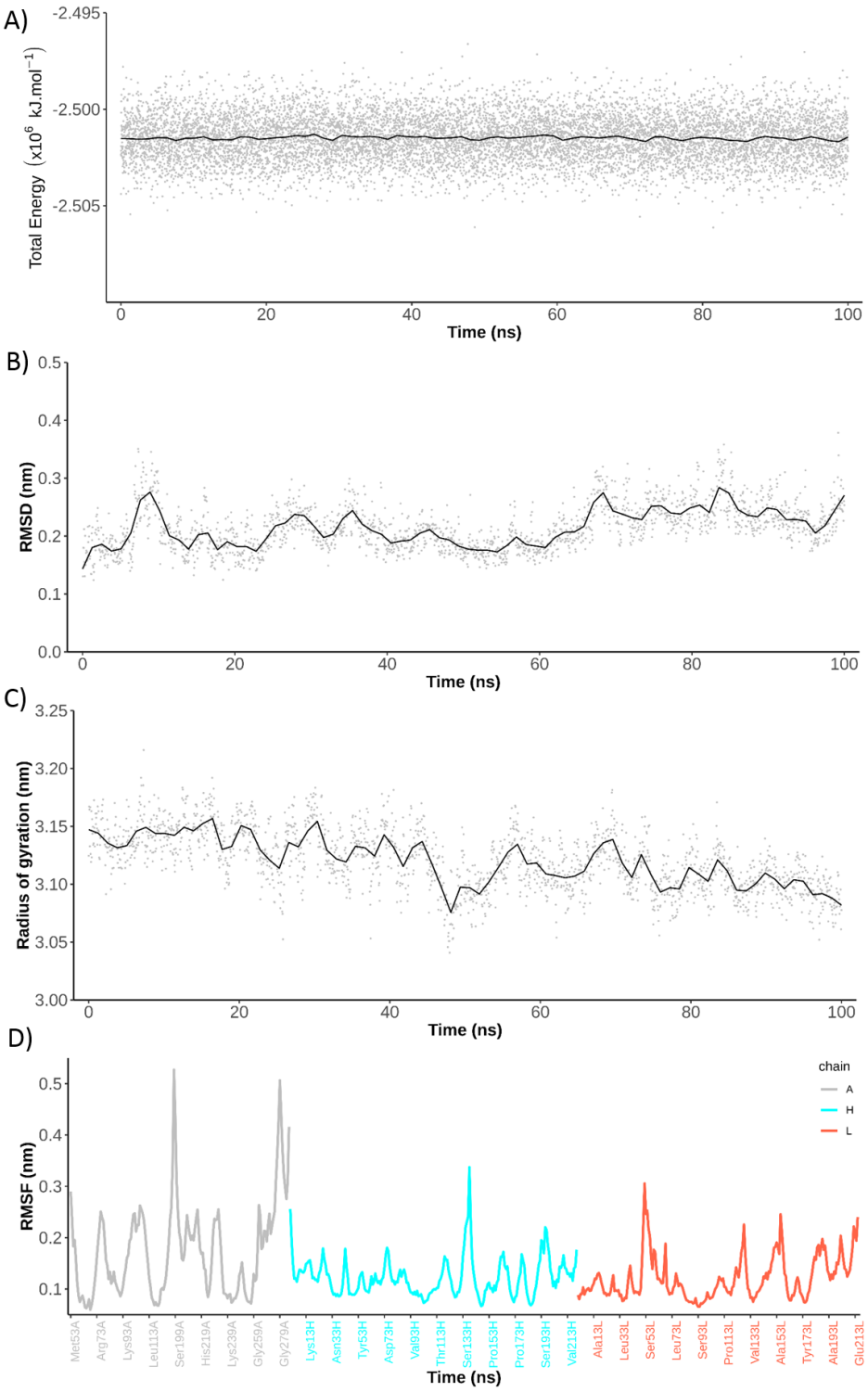

Figure S4 – Diagnostic plots for Lys118Ala system simulation showing the profiles of potential energy (A), root-mean-square deviation after the superposition of C_α atoms to initial structure (B), gyration radius for all atoms (C) and root-mean square fluctuation of C_α atoms from 80 to 100 ns (D).

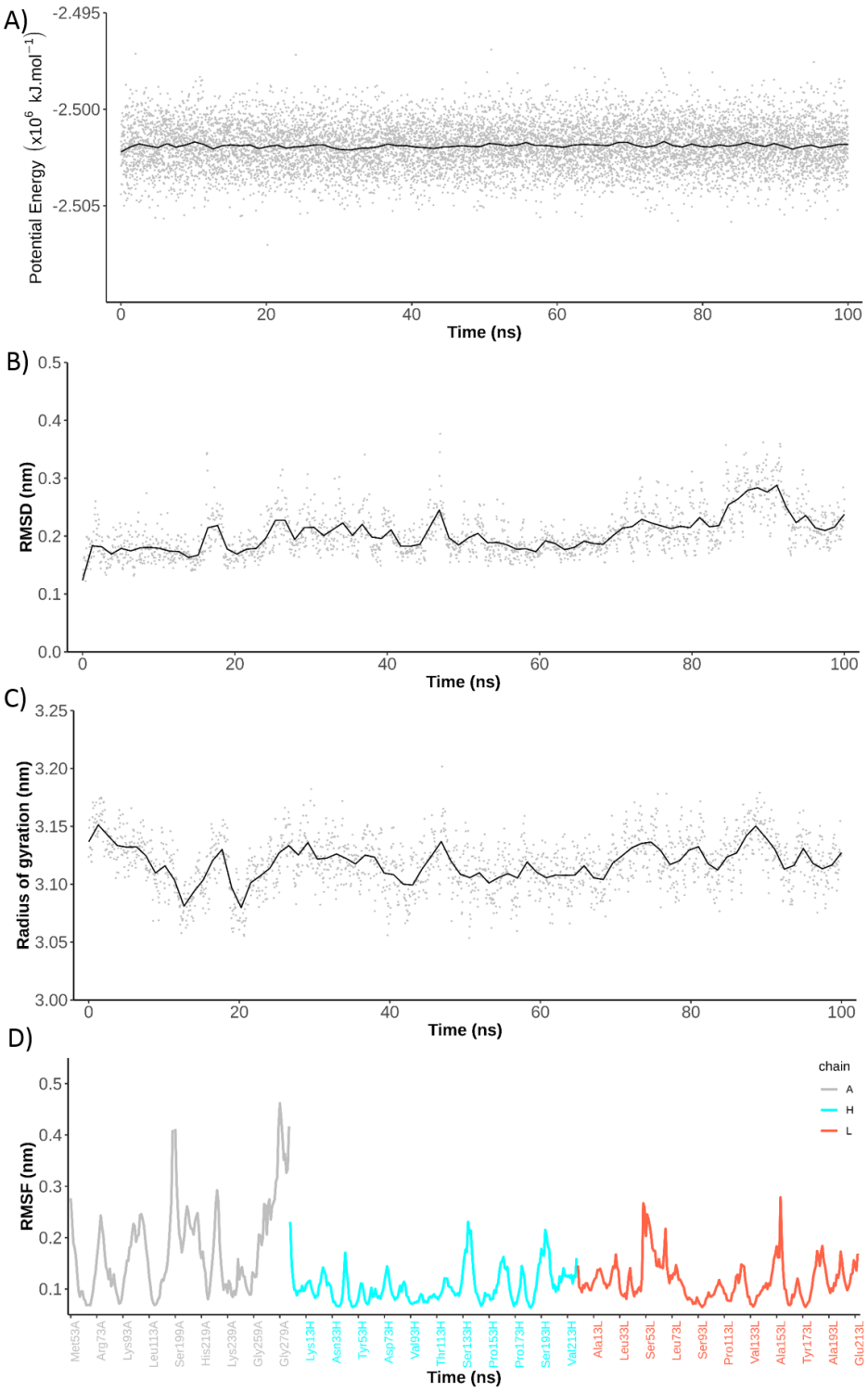

Figure S5 – Diagnostic plots for Asp247Ala system simulation showing the profiles of potential energy (A), root-mean-square deviation after the superposition of C_α atoms to initial structure (B), gyration radius for all atoms (C) and root-mean square fluctuation of C_α atoms from 80 to 100 ns (D).

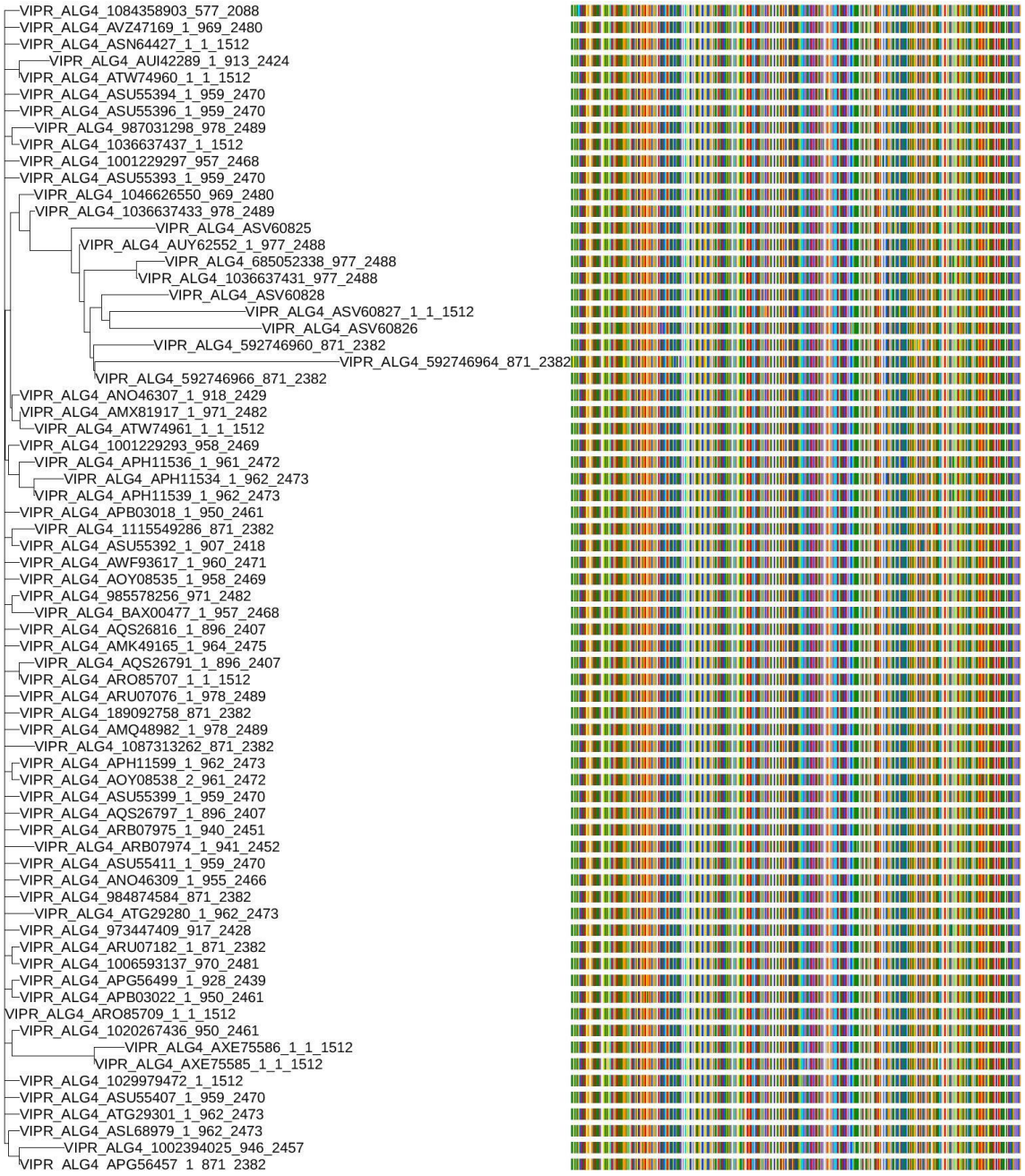

Figure S6 – The phylogenetic tree generated with conservation analysis and the respective alignment matrix for complete sequences of ZIKV sE protein obtained from the *Virus Pathogen Database and Analysis Resource* (https://www.viprbrc.org/).

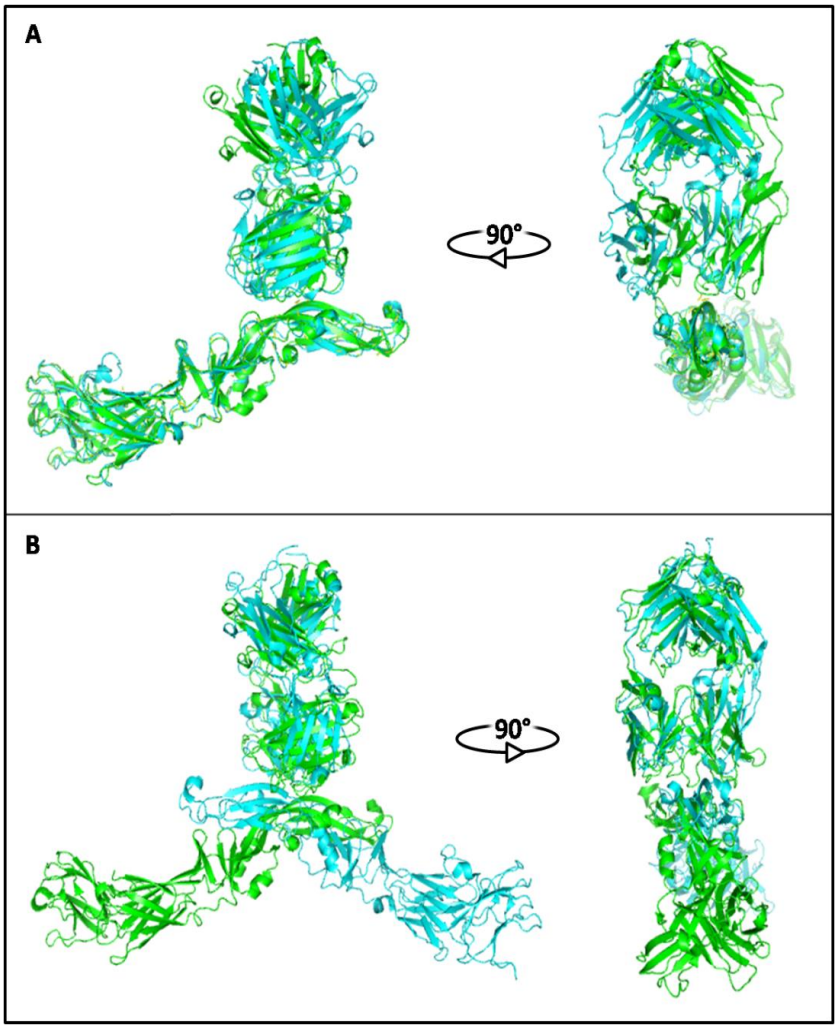

Figure S7 – Complexes formed by Z20 (green) and ZIKV-117 (cyano) on the ZIKV envelope protein showing the overlap of only the E (A) and Fab (B) regions, indicating the two antibodies are in different orientations in relation to protein E.

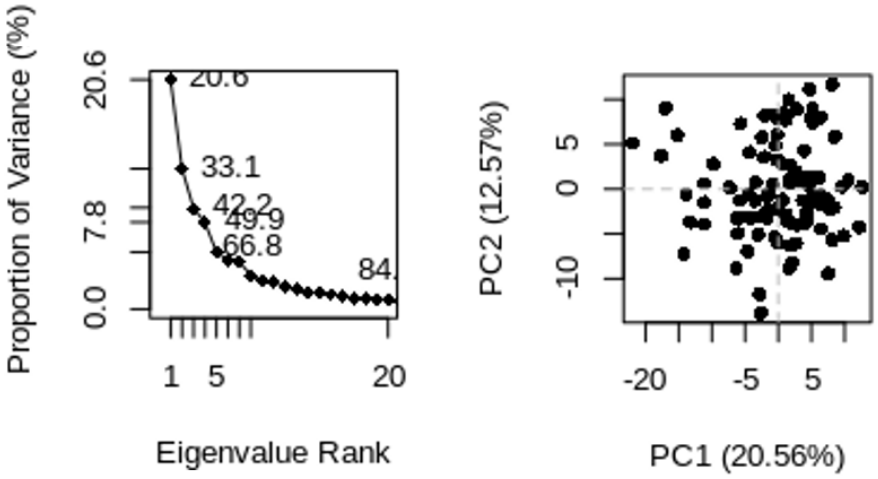

Figure S8 – Principal component analysis results showing the proportion of variance along the first 20 components (left) and the 2D distribution of the first two components (right).

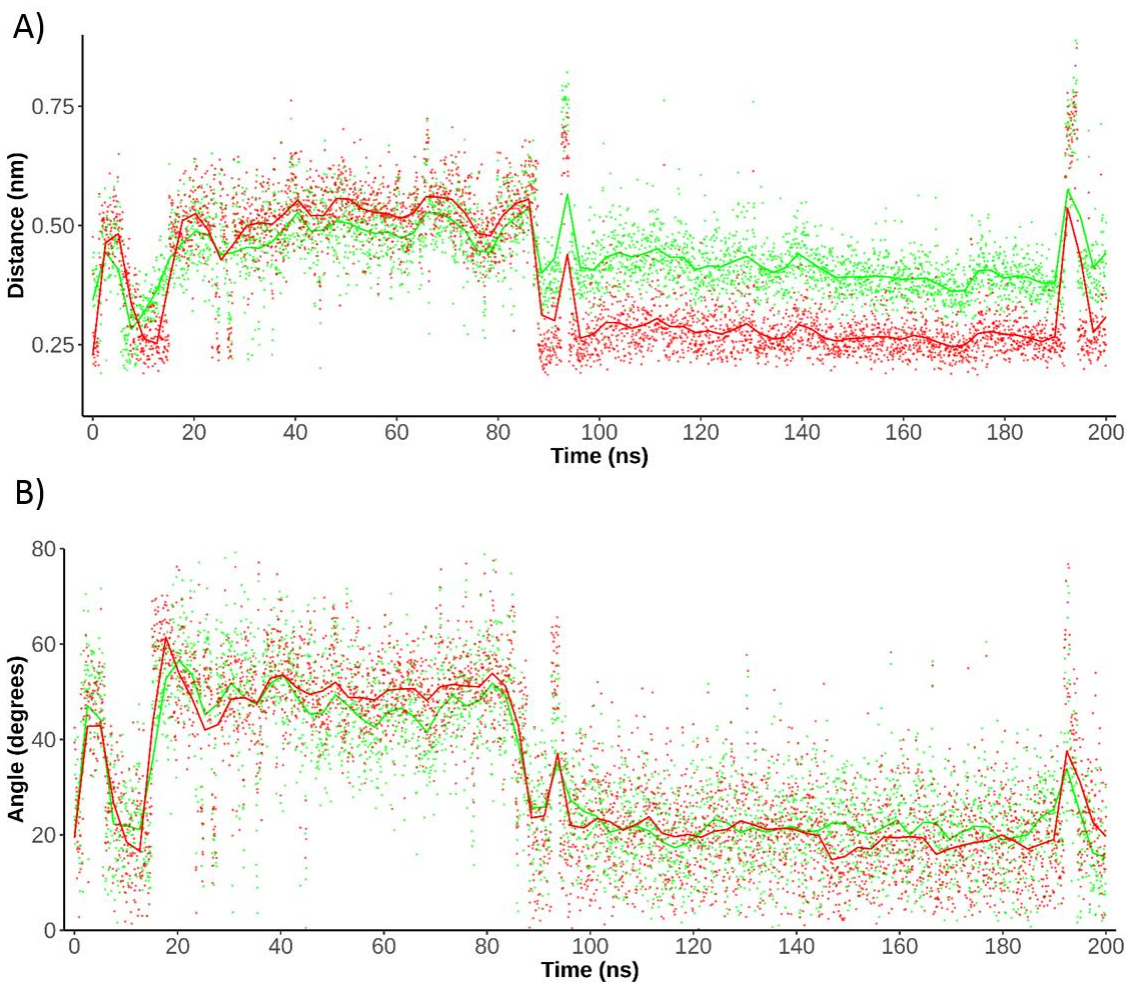

Figure S9 –Profiles of the distances (A) and angles (B) showing the dynamic of the cation-π interaction between the residues Gln89A and Tyr53H. The distances were calculated between the hydrogen atoms 1HE2 (green) and 2HE2 (red) of the amino group of the side chain of Gln89A with the center of mass of the aromatic ring of the side chain of Tyr53H. The respective angles were calculated between the normal vector from the plane of the aromatic ring and the vector from the center of mass of aromatic ring to 1HE1 (green) and 2HE2 (red).

Table S1 – PDB codes of the structures whose sequences have 100% identity and total coverage in relation to the consensus sequence of sE

PDB id (chain)	Coverage	Identity (%)	X-ray resolution
5JHM (A e B)	1.0	100	2.0 Å
5LBV (A)	1.0	100	2.2 Å
5GZN (A)	1.0	100	3.0 Å
5GZO (D)	1.0	100	2.8 Å
5JHL (A)	1.0	100	3.0 Å
5LBS	1.0	100	2.2 Å

Table S2 - The contribution for van der Waals (vdW), electrostatic (Elec), polar solvation (Polar) and non-polar solvation (Nonpolar) of estimated free energies for the residue pairs (ΔG_{pair}) selected with $\Delta G_{pair} < -1$ kcal.mol^{-1}, the occurrence of hydrogen bonds showing between parenthesis the de number of individual donor-acceptor pairs, the normalized conservation scores for the EDII position and the residues variety at each position of the multiple sequence alignment. The energy terms are in kcal.mol^{-1}

EDII residue	Z20 residue	vdW	Elec	Polar	Nonpolar	ΔG_{pair}	Occurrence (%)	Normalized conservation score	Residue variety
Ser64A	Asp102H	0.2 ± 0.8	-5.8 ± 1.3	3.0 ± 0.4	-0.6 ± 0.1	-3.2 ± 0.8	87.0 (1)	0.80	Ser, Thr
Ser64A	Leu103H	-0.9 ± 0.2	-0.2 ± 0.1	0.1 ± 0.1	-0.6 ± 0.1	-1.7 ± 0.3	-		
Ile65A	Leu103H	-0.7 ± 0.1	0.2 ± 0.1	-0.2 ±0.1	-0.4 ± 0.1	-1.1 ± 0.2	-	2.60	Ile, Lys, Leu
Ile65A	Asn92L	-0.6 ± 0.3	-1.1 ± 1.0	0.7 ± 0.4	-0.5 ± 0.2	-1.5 ± 0.9	-		
Ser66A	Leu103H	-0.7 ± 0.3	-0.4 ± 0.3	0.4 ± 0.2	-0.8 ± 0.1	-1.5 ± 0.3	-	-0.75	Ser
Ser66A	His91L	-0.7 ± 0.5	1.0 ± 1.6	-1.3 ± 1.1	-0.7 ± 0.1	-1.6 ± 0.8	0.2 (1)		
Ser66A	Asn92L	-0.9 ± 0.2	-0.2 ±0.3	-0.1 ± 0.2	-0.5 ± 0.1	-1.7 ± 0.4	-		
Asp67A	His91L	-0.6 ± 0.1	-18.7 ± 1.1	18.0 ± 0.9	-0.3 ± 0.0	-1.5 ± 0.4	75.4 (1)	-0.57	Asp
Asp67A	Asn92L	-0.7 ± 0.2	0.4 ± 0.6	-0.4 ± 0.6	-0.3 ± 0.0	-1.0 ± 0.3	-		
Asp67A	Tyr94L	-1.3 ± 0.2	-2.5 ± 0.4	2.5 ± 0.4	-0.9 ± 0.1	-2.2 ± 0.3	-		
Asp67A	Arg96L	-0.3 ± 0.3	-32.7 ± 6.2	30.0 ± 2.5	-0.3 ± 0.2	-3.3 ± 4.0	-		
Met68A	Asn92L	-0.4 ± 0.5	-2.1 ± 0.6	0.3 ± 0.3	-0.7 ± 0.1	-2.9 ± 0.6	98.7 (1)	2.53	Ile, Met, Thr
Met68A	Ser93L	-1.4 ± 0.3	-1.2 ± 1.0	0.2 ± 0.5	-1.0 ± 0.1	-3.3 ± 0.5	-		
Met68A	Tyr94L	-0.7 ± 0.3	-1.2 ± 0.5	-0.1 ± 0.2	-0.4 ± 0.1	-2.5 ± 0.3	-		
Ala69A	Tyr94L	-0.5 ± 0.1	-0.3 ± 0.1	0.2 ± 0.0	-0.6 ± 0.1	-1.2 ± 0.2	-	2.48	Val, Ala, Thr
Lys84A	Asn59H	-0.1 ± 0.4	-6.4 ± 2.9	4.3 ± 1.7	-0.6 ± 0.2	-2.9 ± 1.3	43.4 (1)	1.44	Arg, Lys
Gln89A	Trp34H	-0.9 ± 0.3	-0.6 ± 1.3	0.2 ± 0.8	-0.8 ± 0.1	-2.1 ± 0.8	1.1 (1)	-0.57	Gln
Gln89A	Tyr53H	-1.1 ± 0.2	-0.7 ± 0.5	0.1 ± 0.4	-0.8 ± 0.1	-2.6 ± 0.6	0.1 (1)		

Table S2 (continued).

EDII residue	Z20 residue	v.d.W	Elec	Polar	Non Polar	ΔG_{pair}	Occurrence (%)	Normalized conservation score	Residue variety
Lys118A	Trp34H	-1.6 ± 0.2	-2.4 ± 0.9	-0.6 ± 0.7	-1.4 ± 0.1	-5.9 ± 1.0	4.6 (1)	-0.51	Lys
Lys118A	Glu51H	0.8 ± 0.7	-53.5 ± 1.8	41.2 ± 0.8	-0.5 ± 0.0	-12.0 ± 1.2	98.2 (2)		
Lys118A	Leu103H	-1.0 ± 0.3	0.2 ± 0.3	-0.2 ± 0.3	-0.9 ± 0.1	-2.0 ± 0.3	-		
Ala120A	Leu103H	-0.6 ± 0.5	0.0 ± 0.0	0.0 ± 0.0	-0.7 ± 0.1	-1.3 ± 0.5	-	0.90	Ala, Thr
Ser122A	Asp102H	-0.6 ± 0.2	-0.3 ± 1.1	0.3 ± 1.0	-0.6 ± 0.2	-1.2 ± 0.4	0.1 (1)	0.85	Ser, Cys
Gly232A	His54H	-0.3 ± 0.3	-3.0 ± 1.8	2.6 ± 1.4	-0.3 ± 0.2	-1.0 ± 0.8	3.3 (1)	-0.38	Gly
Thr233A	Tyr53H	-0.6 ± 0.3	-0.1 ± 0.4	0.0 ± 0.1	-0.5 ± 0.2	-1.2 ± 0.6	7.5 (1)	-0.70	Thr
Lys246A	Arg30L	-1.2 ± 0.4	28.6 ± 3.0	-27.9 ± 2.8	-1.0 ± 0.3	-1.6 ± 0.5	-	1.14	Arg, Lys
Asp247A	Arg30L	0.6 ± 0.8	-50.5 ± 2.1	39.9 ± 0.9	-0.8 ± 0.1	-10.8 ± 1.3	100.0 (3)	1.05	Asp, Glu
Arg252A	Gln27L	-0.9 ± 0.5	0.4 ± 2.9	-0.5 ± 2.3	-0.9 ± 0.4	-1.8 ± 1.2	7.7 (3)	1.10	Arg, Thr
Arg252A	Gly28L	0.0 ± 0.4	-4.4 ± 3.6	2.5 ± 1.4	-0.2 ± 0.2	-2.1 ± 2.4	37.0 (2)		
Thr254A	Ile29L	-0.6 ± 0.2	-0.2 ± 0.2	0.2 ± 0.1	-0.4 ± 0.2	-1.1 ± 0.3	-	-0.70	Thr
Thr254A	Arg30L	-0.8 ± 0.2	2.2 ± 0.7	-1.7 ± 0.5	-0.7 ± 0.1	-1.1 ± 0.4	0.3 (1)		
Val255A	Asn31L	-0.1 ± 0.3	-1.6 ± 1.2	0.3 ± 0.3	-0.2 ± 0.1	-1.6 ± 1.1	56.1 (1)	0.92	Val, Ala
Val256A	Arg30L	-0.8 ± 0.2	0.2 ± 0.2	-0.3 ± 0.2	-0.8 ± 0.1	-1.7 ± 0.3	-		